The contribution of metabolic and adipose tissue inflammation to non-alcoholic fatty liver disease

Mulder, P.C.A.

Chapter 3

Reduction of obesity-associated white adipose tissue inflammation by rosiglitazone is associated with reduced non-alcoholic fatty liver disease in LDLr-deficient mice

Petra Mulder[1,2], Martine C. Morrison[1], Lars Verschuren[3], Wen Liang[1], J. Hajo van Bockel[2], Teake Kooistra[1], Peter Y. Wielinga[1], Robert Kleemann[1,2]

[1] Department of Metabolic Health Research, Netherlands Organization for Applied Scientific Research (TNO), Zernikedreef 9, 2333 CK Leiden, The Netherlands
[2] Department of Vascular Surgery, Leiden University Medical Center, PO Box 9600, 2300 RC Leiden, The Netherlands
[3] Department of Microbiology and Systems Biology, Netherlands Organization for Applied Scientific Research (TNO), 3704 HE, Zeist, The Netherlands

Scientific Reports. 2016 Aug 22;6:31542. doi: 10.1038/srep31542

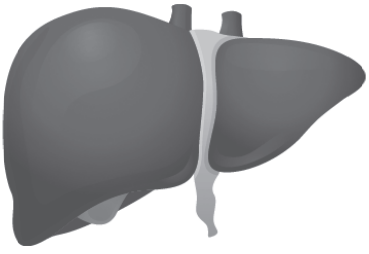

ABSTRACT

Obesity is associated with chronic low-grade inflammation that drives the development of metabolic diseases, including non-alcoholic fatty liver disease (NAFLD). We recently showed that white adipose tissue (WAT) constitutes an important source of inflammatory factors. Hence, interventions that attenuate WAT inflammation may reduce NAFLD development. Male LDLr-/- mice were fed a high-fat diet (HFD) for 9 weeks followed by 7 weeks of HFD with or without rosiglitazone. Effects on WAT inflammation and NAFLD development were analyzed using biochemical and (immuno)histochemical techniques, combined with gene expression analyses. Nine weeks of HFD feeding induced obesity and WAT inflammation, which progressed gradually until the end of the study. Rosiglitazone fully blocked progression of WAT inflammation and activated PPARγ significantly in WAT. Rosiglitazone intervention did not activate PPARγ in liver, but improved liver histology and counteracted the expression of genes associated with severe NAFLD in humans. Rosiglitazone reduced expression of pro-inflammatory factors in WAT (TNFα, leptin) and increased expression of adiponectin, which was reflected in plasma. Furthermore, rosiglitazone lowered circulating levels of pro-inflammatory saturated fatty acids. Together, these observations provide a rationale for the observed indirect hepatoprotective effects and suggest that WAT represents a promising therapeutic target for the treatment of obesity-associated NAFLD.

INTRODUCTION

The prevalence of obesity has increased dramatically over the last 30 years and metabolic disorders associated with obesity have become a major health and economic problem worldwide [1]. Obesity is associated with a state of low-grade chronic inflammation, frequently referred to as systemic inflammation or metabolic inflammation [2], which is thought to drive the development of several metabolic diseases including non-alcoholic fatty liver disease (NAFLD) [3,4]. We recently showed that adipose tissue is a critical source of inflammation in obesity and causally involved in NAFLD progression [5]. However, it is unclear whether suppression of adipose tissue inflammation would attenuate NAFLD progression.

White adipose tissue (WAT) is the primary site of energy storage. This storage function involves expansion of WAT through adipocyte hyperplasia (increase in cell number) and adipocyte hypertrophy (increase in cell size) [6]. Adipocyte hypertrophy is closely associated with WAT inflammation: in an in vitro experiment with isolated primary human adipocytes [7], only very hypertrophic cells were found to secrete MCP-1, a key mediator of immune cell recruitment into WAT. Consistent with this observation, adipocyte hypertrophy is associated with infiltration of macrophages and formation of crown-like structures (CLS) [8], a histological hallmark of inflamed WAT. Notably, a strong increase in CLS is observed at the time point at which a WAT depot has reached its maximal mass as shown very recently in a model of diet-induced obesity [5].

It is thought that the inflamed WAT is less insulin sensitive, which enhances lipolysis of stored fat, thereby contributing to ectopic fat deposition and the development of liver steatosis [9]. In line with this, Kolak and colleagues [10] have shown that obese patients with inflamed WAT have more liver fat than equally obese subjects without WAT inflammation. In addition to the increased fat flux, inflamed WAT may produce inflammatory factors that can contribute to systemic inflammation and promote the progression from liver steatosis to non-alcoholic steatohepatitis (NASH) [2,11,12]. However, experimental support for a causal role of WAT in the development of NASH has long been lacking. Recently we have shown that surgical removal of inflamed abdominal (epididymal) WAT in mice reduced

lobular inflammation and attenuated NASH development [5], suggesting that WAT constitutes an possible target for the treatment of NASH.

WAT inflammation may be reduced via the nuclear hormone receptor peroxisome proliferator-activated receptor-γ (PPARγ) which is predominantly expressed in adipose tissue, controlling inflammatory and metabolic processes [13]. Previous studies in humans [14] and animals [15-17], provide indication that pharmacological activators of PPARγ such as rosiglitazone may reduce the inflammatory state of WAT in obesity. We herein investigated whether rosiglitazone intervention can reduce manifest WAT inflammation and would attenuate subsequent NAFLD development. To do so, we first determined the time point at which WAT inflammation develops during high-fat diet treatment in LDLr-/- mice. Subsequently, we studied the therapeutic effect of rosiglitazone on WAT inflammation and associated NAFLD development.

METHODS

Animal experiments

All animal experiments were approved by the institutional Animal Care and Use Committee of the Netherlands Organization of Applied Scientific Research (Zeist, The Netherlands; approval number DEC2935) and were conducted in accordance with the Dutch Law on Animal Experiments, following international guidelines on animal experimentation. Mice (aged 12-14 weeks at the start of the experiment) had ad libitum access to food and water.

Time-course study: Male LDLr-/- mice were fed a high-fat diet (HFD: 45 kcal% lard fat, D12451, Research Diets, New Brunswick, NJ, USA) and were sacrificed after 0, 9 and 16 weeks to collect epididymal WAT (eWAT), mesenteric WAT (mWAT) and inguinal WAT (iWAT). Tissues were prepared essentially as reported [5].

Intervention study: Tissues and plasma were obtained from a large cohort study in which rosiglitazone and other interventions (e.g. fenofibrate) were analyzed [18]. Briefly, one group (n=9) was sacrificed after 9 weeks of HFD to define the condition prior to intervention (reference, REF). The remaining mice continued on

HFD (HFD, n=13) or HFD supplemented with 0.01% w/w rosiglitazone (HFD+Rosi, n=9, Avandia, GSK, Zeist, The Netherlands). A separate control group was kept on chow as a baseline control for microarray and RT-PCR gene expression analysis. In week 16, all animals were sacrificed and WAT depots and liver were collected. Mice (n=2) that did not become obese after 9 weeks of high-fat feeding (i.e. body weight gain 50% less than group mean), were excluded from the analyses.

Histological, biochemical, metabolomics and gene expression analyses

Briefly, WAT characteristics and NAFLD development were quantified histologically as described [5,19]. Immunohistochemistry was performed on frozen, acetone-fixed WAT sections using primary antibodies specific for CCR2 (PA5-23044, Thermo Fisher Scientific, Rockford, IL, USA) and CD11c (BD553800, BD Biosciences, San Diego, CA, USA). After incubation, biotinylated antibodies were detected by incubation with streptavidin-HRP using Nova Red as a substrate (both, Vector Laboratories, Burlingame, CA, USA). All sections were counterstained with hematoxylin. Immunopositive cells were quantified in four different cross-sections per mouse using ImageJ. Intrahepatic triglyceride concentrations were analyzed by high performance thin-layer chromatography (HPTLC) [18]. Plasma parameters were determined with commercially available assays as previously specified [18]. Plasma fatty acids were determined by gas chromatography/mass spectrometry (GC/MS) [18]. The plasma concentration of total free non-esterified fatty acids (NEFAs) was determined with NEFA-HR kit (Instruchemie, Delfzijl, The Netherlands). Illumina microarray gene expression and subsequent pathway analysis of eWAT and liver was performed following established protocols. To analyze potential off-target effects of rosiglitazone in the liver, an upstream transcriptional activator analysis was performed [20]. Microarray data were validated and confirmed by RT-PCR and changes in expression were calculated using the comparative Ct (ΔΔCt) method, expressed as fold-change relative to chow.

Statistical analysis

All data are presented as mean ± SEM. Data were analyzed using one-way ANOVA and least significant difference (LSD) post-hoc test. Non-normally distributed

data were analyzed by Kruskal-Wallis followed by Mann-Whitney U post-hoc test. Correlations were determined by Spearman's rank correlation. Statistically significant differences in plasma fatty acids over time within HFD and HFD+Rosi were analyzed using Student's paired *t*-test. Statistical tests were performed using Graphpad Prism software (version 6, Graphpad Software Inc., La Jolla, USA). $P<0.05$ was considered statistically significant.

RESULTS

WAT inflammation starts in eWAT during high-fat diet-induced obesity

After 16 weeks, CLS formation was most pronounced in eWAT (Figure 1A), while CLS were hardly observed in mWAT and iWAT. Quantitative analysis showed a marked increase in CLS number in eWAT ($p<0.05$; Figure 1B). CLS number correlated with eWAT mass (r=0.80, $p<0.001$, not shown) and with average adipocyte size, a measure of adipocyte hypertrophy (r=0.61, $p<0.01$; Figure 1C). The average adipocyte size in eWAT was greater than in mWAT and iWAT (not shown). Hence, eWAT is most susceptible to develop CLS, with substantial inflammation established after 9 weeks of high-fat feeding.

Rosiglitazone attenuates WAT inflammation independent of obesity and targets WAT

Mice were treated with high-fat diet for 9 weeks to induce obesity (Table 1). At this time point, intervention with rosiglitazone was started. The caloric intake was comparable between the HFD control group and the HFD+Rosi group (14.6±0.7 and 13.4±0.6 kcal/day, respectively). Continuous high-fat feeding increased fasting plasma glucose, while rosiglitazone had a significant lowering effect (Table 1). Rosiglitazone also significantly lowered fasting plasma insulin and HOMA-IR relative to HFD mice (Table 1). Weight gain and total fat mass were comparable between HFD and HFD+Rosi (Table 1), indicating that the observed metabolic effects were independent of obesity.

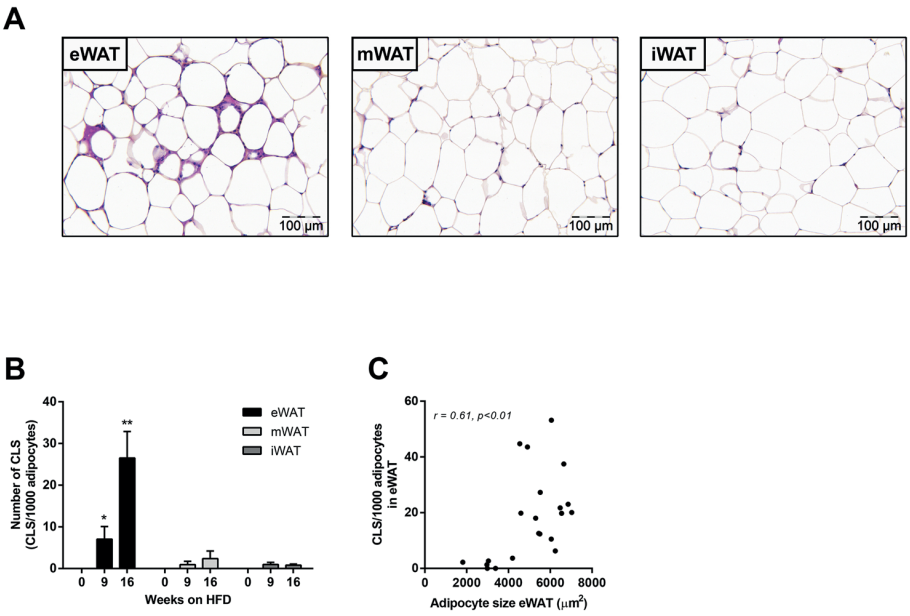

Figure 1. Effect of HFD feeding on development of WAT inflammation. (A) Representative photomicrographs of three WAT depots after 16 weeks of high-fat feeding. (B) Quantitative analysis of CLS formation over time in the major adipose tissue depots, eWAT, mWAT and iWAT. (C) Positive correlation between CLS number and adipocyte size in eWAT. Data are mean±SEM (n=8/group), *p<0.05 compared with t=0; **p<0.05 compared with t=0 and 9 weeks of high-fat feeding.

Table 1 Metabolic parameters of experimental groups

Parameter	Chow	REF	HFD	HFD+Rosi
Body weight gain (g)	3.21 ± 0.48	9.14 ± 1.81*a*	17.49 ± 0.*91b*	17.07 ± 1.*24b*
Total adiposity (g)	1.00 ± 0.11	2.61 ± 0.55*a*	4.41 ± 0.27*b*	4.07 ± 0.28*b*
Glucose (mM)	11.12 ± 0.33	12.52 ± 0.72*a*	15.00 ± 0.48*b*	10.61 ± 0.22*c*
Insulin (ng/ml)	0.65 ± 0.19	2.88 ± 0.80*a*	4.65 ± 0.94*b*	1.40 ± 0.21*c*

Abbreviations: *Chow,* mice fed a chow diet for 16 weeks; *REF,* reference, mice receiving a HFD for 9 weeks to define condition prior to intervention; *HFD,* control mice after 16 weeks of HFD; *HFD+Rosi,* rosiglitazone-treated mice (intervention from 9-16 weeks). *a,* Significantly different from chow; *b,* Significantly different from chow and REF; *c,* Significantly different from HFD (all, p<0.05).

Quantification of CLS in eWAT revealed that CLS numbers were increased in HFD relative to REF, but remained constant in HFD+Rosi (Figure 2A). Hence, rosiglitazone fully blocked further CLS formation but did not resolve existing inflammation (Figure 2B). These effects were paralleled by decreased gene expression of MCP-1 in HFD+Rosi (Figure 2C). Gene expression of macrophage markers revealed that rosiglitazone intervention reduced the pro-inflammatory M1 macrophage markers CD11c and CCR2 (Figure 2D). In addition, rosiglitazone increased the expression of anti-inflammatory M2 macrophage marker Arginase-1, but did not affect CD206 (Figure 2D). Consistent with this, we found less immunoreactivity against CCR2 and CD11c in adipose tissue of mice treated with rosiglitazone as determined by immunohistochemical analysis (Supplement 1). Refined analysis of CLS revealed that CLS contain CCR2+ and CD11c+ cells and some cells expressed both markers in the HFD group as well as the HFD+Rosi group (Supplement 1). Furthermore, rosiglitazone influenced the expression of genes involved in inflammatory and oxidative stress pathways as shown by microarray analysis (Supplement 2). The observed reduction of eWAT inflammation in HFD+Rosi mice was paralleled by a decreased adipocyte size (Figure 2E).

To validate that rosiglitazone affected PPARγ-regulated genes in eWAT under the experimental conditions employed an upstream transcriptional regulator analysis was performed. This analysis demonstrated a highly significantly increased transcriptional activity of PPARγ (Z-score: 4.1, p=5.92e-24). More specifically, rosiglitazone significantly affected the expression of 1049 genes (FDR<0.05), of which 71 are established PPARγ-regulated genes (including fatty acid transporter protein 1, fatty acid binding proteins, perilipin, uncoupling protein-1, acyl-CoA synthetase) (for detailed list, see Supplement 2). By contrast, microarray analysis of corresponding livers under the same statistical cut-off (FDR<0.05) revealed that only 36 genes (among which 4 PPARγ-regulated genes) were differentially expressed by rosiglitazone (Supplement 3), and upstream transcriptional regulator analysis showed no activation of PPARγ. There were also no indications for off-target activation of PPARα or PPARδ from this microarray analysis (Supplement 3). Altogether, these data demonstrated that rosiglitazone significantly activated PPARγ in WAT and attenuated high-fat diet induced WAT inflammation.

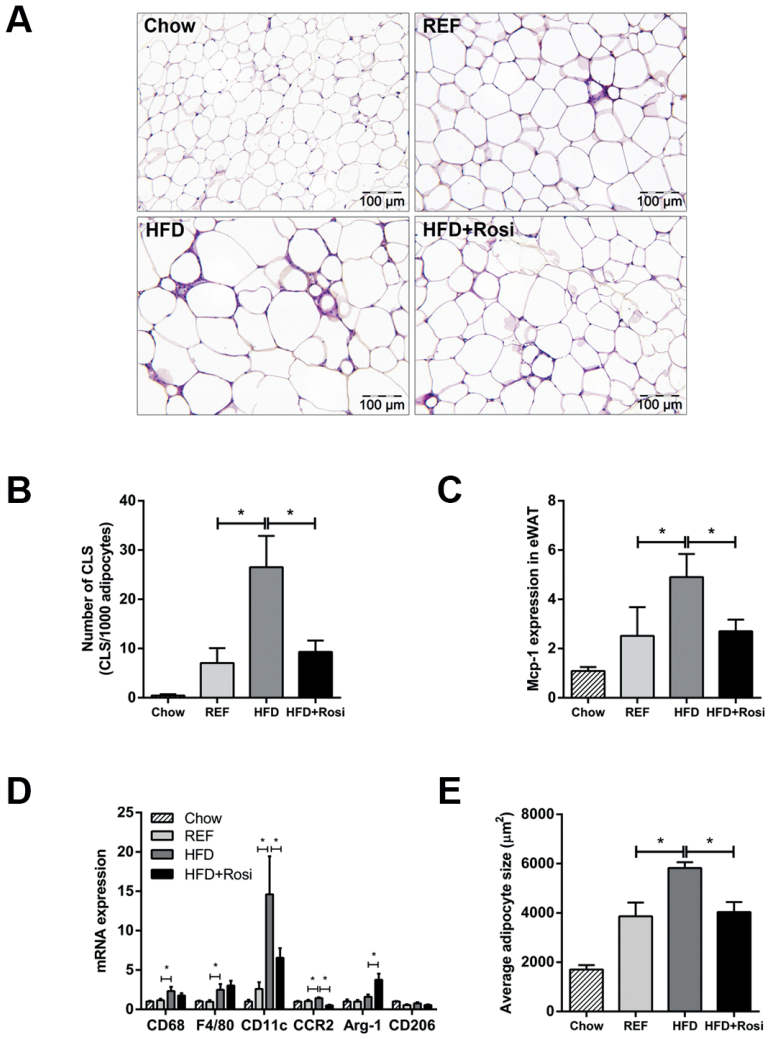

Figure 2. Effects of rosiglitazone intervention on eWAT inflammation. (A) Representative photomicrographs of HPS-stained eWAT cross-sections (magnification x200). (B) High-fat feeding strongly increased CLS formation in eWAT between 9 weeks (REF) and 16 weeks (HFD), while rosiglitazone fully blocked further CLS formation. (C) MCP-1 gene expression was increased in HFD mice, but not in HFD+Rosi. (D) Gene expression of macrophage markers. Rosiglitazone reduced HFD-induced expression of M1 markers (CD11c and CCR2) and increased gene expression of M2 marker Arginase-1 (Arg-1). HFD-induced expression of general macrophage markers, Cd68 and F4/80, was not affected by rosiglitazone. (E) Morphometric analysis of average adipocyte size revealed that rosiglitazone attenuated HFD-induced increase in adipocyte size in eWAT. Data are mean±SEM (n=7-10/group), *p<0.05. Mean expression of RT-PCR data was set 1 for chow-fed mice.

Rosiglitazone prevents progression of NAFLD

Next, we investigated the effects of rosiglitazone intervention on the liver. High-fat feeding resulted in mild/moderate hepatic steatosis after 9 weeks (REF), which was markedly aggravated after 16 weeks (HFD) (Figure 3A). Rosiglitazone blunted the progression of NAFLD and livers resembled those of REF. Biochemical intrahepatic triglyceride analysis showed a significant increase in HFD relative to REF and liver triglyceride concentrations tended to be lower in HFD+Rosi (Figure 3B). Histological analysis revealed a strong increase in microvesicular steatosis in HFD compared with REF and rosiglitazone fully prevented this increase (Figure 3C). Macrovesicular steatosis, a hallmark of NASH in humans [21], was also elevated in HFD and reduced by rosiglitazone (Figure 3D). High-fat treatment activated several pro-inflammatory and pro-fibrotic pathways in liver including those induced by TNFα (Z-score: 2.79; *p*=3.8e-03), IL-6 (Z-score: 2.03; *p*=2.9e-07) and TGFβ1 (Z-score: 1.3; *p*=1.38e-05) as demonstrated by pathway analysis (FDR<0.05). Moreover, high-fat treatment induced several genes which were recently identified in human NASH/fibrosis patients [22] (Table 2). Rosiglitazone treatment attenuated this effect and counteracted the expression of genes including Col14A1, TaxIBP3, EFEMP2, EGFBP7, THBS2, BICC1 and DKK3. Furthermore, RT-PCR analysis of TNFα, which plays an essential role in NASH, showed increased TNFα gene expression in HFD mice and that rosiglitazone treatment quenched this induction (Figure 3E). Similarly, HFD-induced expression of pro-fibrotic genes Col1a1, Col1a2 and TIMP-1 were suppressed by rosiglitazone intervention (Figure 3F). High-fat feeding also resulted in infiltration of neutrophils (MPO-positive inflammatory cells) and formation of inflammatory cell aggregates characteristic for NASH [23] between 9 and 16 weeks which was attenuated by rosiglitazone (Supplement 4). Analysis of Sirius-red stained liver cross-sections of the HFD group revealed onset of perisinusoidal fibrosis, which was not observed in HFD+Rosi (Figure 3G). Altogether, intervention with rosiglitazone attenuated the progression from steatosis to NASH.

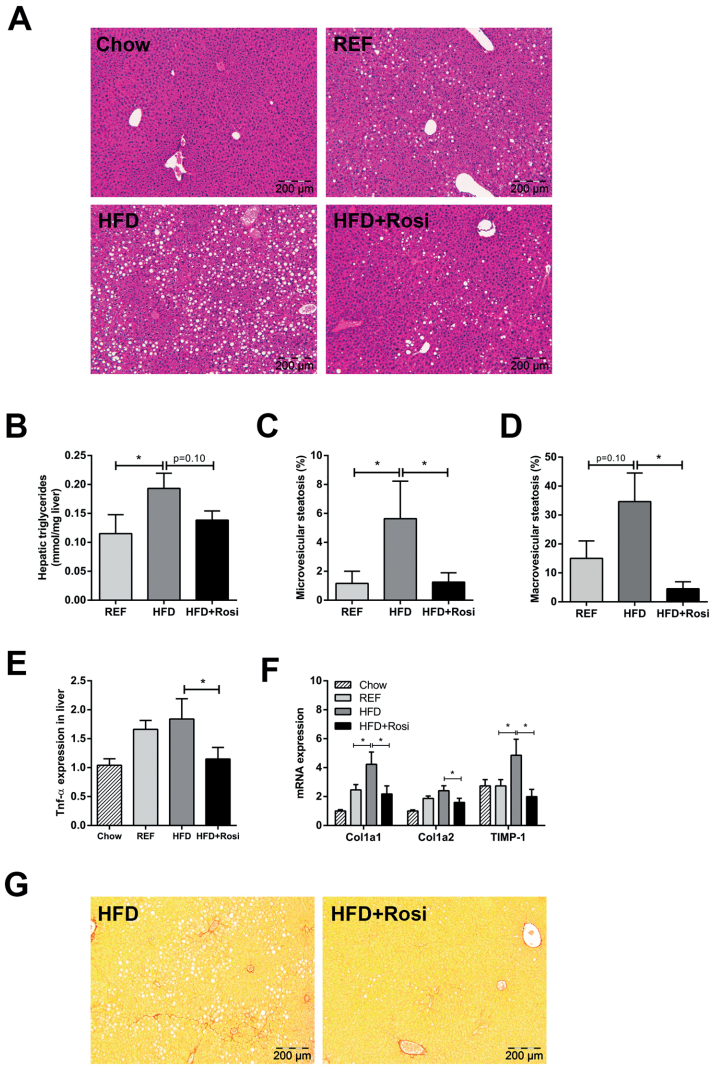

Figure 3. Effects of rosiglitazone intervention on NAFLD development. (A) Representative photomicrographs of HE-stained liver sections of REF, HFD and HFD+Rosi. (B) Biochemical analysis of hepatic triglyceride content. Histological quantification of (C) microvesicular steatosis and (D) macrovesicular steatosis show that steatosis was ameliorated with rosiglitazone compared with HFD (n=7-10/group). (E) TNFα gene expression in liver was diminished in rosiglitazone-treated mice (n=7-8/group). (F) Gene expression of fibrotic genes determined by RT-PCR. Rosiglitazone reduced HFD-induced expression of Col1a1, Col1a2 and TIMP-1. (G) Onset of fibrosis in Sirius Red-stained liver cross-sections in HFD mice, but not in HFD+Rosi. Pictures are shown in magnification x100. Data are mean±SEM, *p<0.05. Mean expression of RT-PCR data was set 1 for chow-fed mice.

Table 2. Microarray analysis of hepatic gene expression profile based on genes identified in human NAFLD

			HFD vs Chow			HFD+Rosi vs HFD		
probeID	**Gene symbol**	**Gene name**	**Fold-Change**		**p-value**	**Fold-Change**		**p-value**
ILMN_2635229	Thbs2	thrombospondin 2	1,740	↑	9,47E-06	0,650	↓	4,62E-04
ILMN_2764588	Igfbp7	insulin-like growth factor binding protein 7	1,465	↑	1,79E-05	0,834	↓	3,52E-02
ILMN_1217309	Tax1bp3	Tax1 (human T-cell leukemia virus type I) binding protein 3	1,360	↑	7,45E-04	0,826	↓	3,28E-02
ILMN_2866901	Efemp2	epidermal growth factor-containing fibulin-like extracellular matrix protein 2	1,556	↑	7,62E-04	0,751	↓	2,70E-02
ILMN_2636424	Itgbl1	integrin, beta-like 1	1,528	↑	1,11E-03	0,905		4,33E-01
ILMN_2746556	Dkk3	dickkopf homolog 3 (Xenopus laevis)	1,402	↑	1,16E-03	0,744	↓	4,27E-03
ILMN_1258629	Col3a1	collagen, type III, alpha 1	1,887	↑	1,61E-03	0,746		1,39E-01
ILMN_2939138	Bicc1	bicaudal C homolog 1 (Drosophila)	1,460	↑	2,69E-03	0,666	↓	1,28E-03
ILMN_2746086	Tax1bp3	Tax1 (human T-cell leukemia virus type I) binding protein 3	1,334	↑	2,94E-03	0,787	↓	1,27E-02
ILMN_2980663	Aqp1	aquaporin 1	0,812	↓	7,68E-03	1,158	↑	5,74E-02
ILMN_2606210	Dpt	dermatopontin	1,459	↑	1,08E-02	0,714	↓	2,26E-02
ILMN_3007428	Sox9	SRY-box containing gene 9	0,694	↓	1,11E-02	1,245		1,23E-01
ILMN_2831656	Epha3	Eph receptor A3	1,334	↑	1,76E-02	0,901		3,84E-01
ILMN_2687872	Col1a1	collagen, type I, alpha 1	1,471	↑	3,99E-02	0,921		6,58E-01
ILMN_2747959	Dcn	decorin	1,151	↑	4,22E-02	0,874	↓	5,21E-02
ILMN_2591027	Col14a1	collagen, type XIV, alpha 1	1,176	↑	4,74E-02	0,820	↓	1,61E-02
ILMN_1223552	Fbn1	fibrillin 1	1,181		6,25E-02	0,885		1,69E-01
ILMN_1233545	Lbh	limb-bud and heart	0,782		6,40E-02	1,089		5,19E-01
ILMN_2669189	Lima1	LIM domain and actin binding 1	1,226		8,23E-02	0,956		6,98E-01
ILMN_1253806	Col1a2	collagen, type I, alpha 2	1,278		8,24E-02	0,837		2,08E-01
ILMN_2852957	Dkk3	dickkopf homolog 3 (Xenopus laevis)	1,184		8,82E-02	0,941		5,38E-01
ILMN_1214954	Cldn10	claudin 10	0,836		1,39E-01	1,143		2,68E-01
ILMN_1228374	Lima1	LIM domain and actin binding 1	1,190		1,48E-01	0,916		4,66E-01
ILMN_2980661	Aqp1	aquaporin 1	0,895		1,89E-01	1,124		1,65E-01
ILMN_1226183	Antxr1	anthrax toxin receptor 1	1,211		1,91E-01	0,815		1,63E-01

Table 2. Microarray analysis of hepatic gene expression profile based on genes identified in human NAFLD (continued)

			HFD vs Chow		HFD+Rosi vs HFD		
probeID	Gene symbol	Gene name	Fold-Change	p-value	Fold-Change		p-value
ILMN_2848305	Pnma1	paraneoplastic antigen MA1	1,144	1,96E-01	0,993		9,43E-01
ILMN_2666018	Mgp	matrix Gla protein	1,162	1,99E-01	0,914		4,39E-01
ILMN_2816180	Lbh	limb-bud and heart	1,137	2,24E-01	0,902		3,29E-01
ILMN_1257077	Jag1	jagged 1	1,160	2,33E-01	0,941		6,22E-01
ILMN_2734683	Fstl1	follistatin-like 1	1,119	2,71E-01	0,949		6,11E-01
ILMN_2596346	Dcn	decorin	1,102	3,26E-01	0,834		6,82E-02
ILMN_2597515	Ehf	ets homologous factor	1,147	3,35E-01	1,055		7,05E-01
ILMN_3001540	Lum	lumican	1,101	4,53E-01	0,817		1,17E-01
ILMN_1227817	Ank3	ankyrin 3, epithelial	1,109	4,57E-01	0,940		6,58E-01
ILMN_2769479	Lama2	laminin, alpha 2	1,116	4,87E-01	0,968		8,38E-01
ILMN_2893417	Sox4	SRY-box containing gene 4	0,929	5,57E-01	0,965		7,75E-01
ILMN_1223963	Ank3	ankyrin 3, epithelial	1,081	5,62E-01	0,835		1,83E-01
ILMN_2836637	Glt8d2	glycosyltransferase 8 domain containing 2	1,078	5,91E-01	1,229		1,45E-01
ILMN_1249021	Bcl2	B-cell leukemia/lymphoma 2	1,058	5,99E-01	0,937		5,50E-01
ILMN_1229643	Antxr1	anthrax toxin receptor 1	1,066	6,02E-01	0,779	↓	4,37E-02
ILMN_2620563	Nexn	nexilin	1,081	6,07E-01	0,771		8,88E-02
ILMN_1238000	Srpx	sushi-repeat-containing protein	1,056	6,75E-01	1,095		4,83E-01
ILMN_2621643	Col4a1	collagen, type IV, alpha 1	1,044	7,12E-01	1,125		3,12E-01
ILMN_2629486	Srpx	sushi-repeat-containing protein	0,958	7,70E-01	0,832		2,12E-01
ILMN_2686036	Tax1bp3	Tax1 (human T-cell leukemia virus type I) binding protein 3	1,030	8,04E-01	1,004		9,72E-01
ILMN_2701712	Plcxd3	phosphatidylinositol-specific phospholipase C, X domain containing 3	0,982	8,80E-01	0,943		6,22E-01
ILMN_2629804	Epha3	Eph receptor A3	0,987	9,04E-01	1,100		3,67E-01

The table lists the genes that were recently reported to be associated with NAFLD severity in humans.[19] HFD feeding of LDLr-/- mice resulted in a significant effect on 16 genes compared to chow (arrows indicate significant up- (↑) or downregulation (↓)). Rosiglitazone counteracted the effect of a HFD as shown by the comparison of HFD+Rosi vs. HFD.

Rationale for the hepatoprotective effects of rosiglitazone

In eWAT, rosiglitazone blocked the HFD-induced gene expression of leptin and TNFα (Figure 4A, B). These effects were paralleled in plasma; HFD+Rosi reduced concentrations of leptin and TNFα (Supplement 5). By contrast, rosiglitazone fully restored the high-fat induced decrease in adiponectin gene expression in eWAT (Figure 4C) which was also reflected in plasma (Supplement 5). In addition, rosiglitazone prevented the high-fat diet-induced increase in total saturated fatty acids in plasma (Figure 4D). In line with this, total NEFA were significantly increased (by 26%, $p<0.05$) in the HFD group, whereas no significant increase was observed in the HFD+Rosi group (11%, n.s.). More specifically, plasma concentrations of palmitic acid (C16:0) and stearic acid (C18:0) were not increased in HFD+Rosi (Figure 4D).

Since WAT inflammation correlated with WAT mass and adipocyte hypertrophy we analyzed effects of rosiglitazone on eWAT, iWAT and mWAT in more detail (Figure 4E). During intervention with rosiglitazone, eWAT mass did not further increase while iWAT mass almost doubled, indicating a shift of fat mass from eWAT towards iWAT. Despite the increase in iWAT mass, this depot did not become inflamed (Figure 4F). Quantification of adipocyte size showed that the expansion in iWAT was mainly attributable to an increase in adipocyte number rather than adipocyte size (Figure 4G). This suggests that increased capability of iWAT to store fat may prevent the development of hypertrophy and associated inflammation in eWAT, and may thereby contribute to beneficial effects of rosiglitazone on NAFLD development.

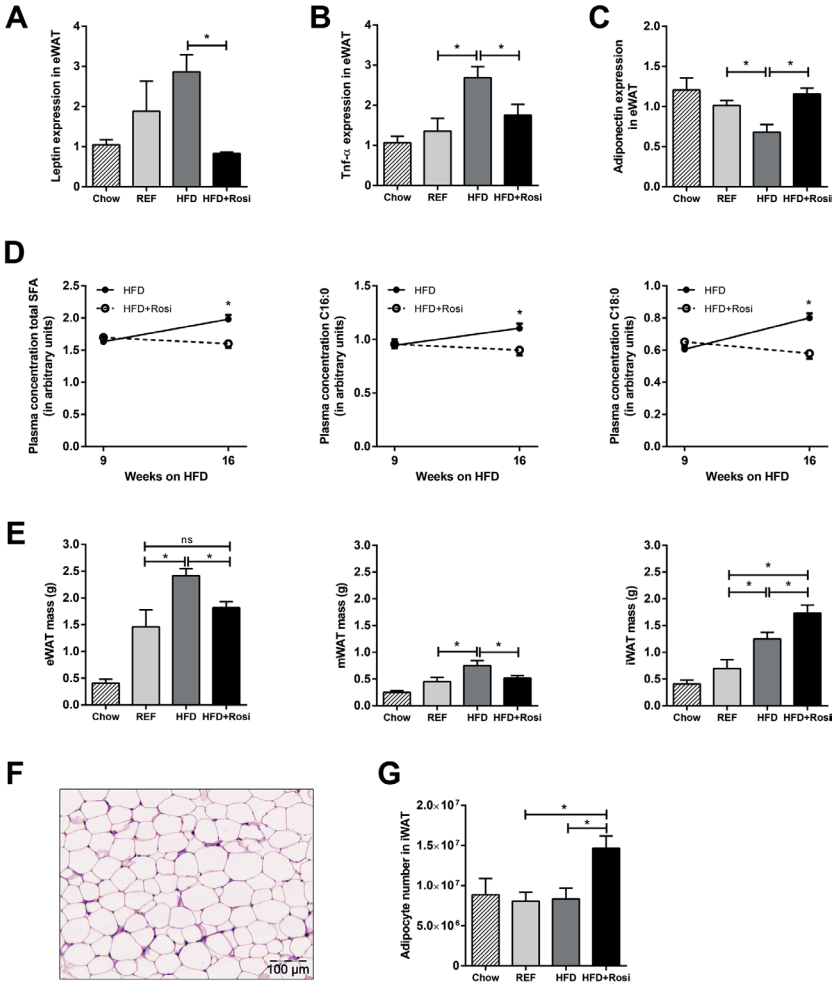

Figure 4. Effects of rosiglitazone on adipokine expression in eWAT, pro-inflammatory fatty acids in plasma and WAT morphology. High-fat feeding increased gene expression in eWAT of pro-inflammatory adipokines (A) leptin, (B) TNFα and decreased expression of (C) anti-inflammatory adipokine adiponectin, while rosiglitazone counteracted these effects. (D) Plasma levels of total saturated fatty acids (SFA) and specific SFAs, palmitic acid (C16:0) and stearic acid (C18:0), were increased between week 9 and 16 of high-fat feeding. This increase was blunted by rosiglitazone (all $p<0.01$; paired t-test; n=9-12/group). (E) The mass of WAT depots was increased in HFD, while rosiglitazone specifically increased iWAT mass. (F) Representative photomicrograph of iWAT in HFD+Rosi, showing absence of CLS. (G) Expansion of iWAT mass in HFD+Rosi was mainly attributable to an increase in adipocyte number. Data are mean±SEM, *$p<0.05$. Mean expression of RT-PCR data was set 1 for chow-fed mice (n=7-8/group). Fatty acid plasma concentration was expressed as arbitrary units relative to internal standard.

DISCUSSION

Recent findings indicate that inflamed (abdominal) WAT plays a causal role in the development of NASH in the context of obesity [5]. WAT may thus constitute a new target for intervention. Compounds that specifically target and quench WAT inflammation have not been developed yet. We therefore used rosiglitazone, an activator of PPARγ with reported anti-inflammatory properties [14-16], as a model compound to intervene in manifest WAT inflammation. Here, we show that rosiglitazone attenuates WAT inflammation and reduces NASH development.

Under the experimental conditions employed herein, rosiglitazone activated PPARγ in WAT, but not in liver, based on a comprehensive analysis of PPARγ-regulated genes. The significant activation of PPARγ in WAT may be important for the observed hepatoprotective effects, because PPARγ activation in liver could cause detrimental effects: Recent knock-out studies have shown that targeted PPARγ deletion in hepatocytes or macrophages protected mice against high-fat induced steatosis [24], while deletion of PPARγ in adipose tissues increased liver steatosis upon high-fat feeding [25]. Furthermore, rosiglitazone treatment remained effective in mice lacking PPARγ specifically in the liver,[26] supporting the view that adipose tissue is an important site of thiazolidinedione action. Consistent with our findings, beneficial effects of rosiglitazone in NAFLD were also observed in aged (12 months old) LDLr-/- mice that develop a more severe disease phenotype than young mice (3 months old) as used herein [27]. However, this study did not examine the effects of rosiglitazone in a therapeutic (intervention) setting and its effects in adipose tissue were not analyzed. In the study by Gupte and colleagues [27], the diet was supplemented with cholesterol which may explain some of the differences observed on liver gene expression and inflammation. Dietary cholesterol has been shown to be a strong inducer of inflammatory gene expression in the liver [28,29]. For instance, treatment with a HFD supplemented with small amounts (0.2% w/w) of cholesterol triggered Kupffer cell activation and inflammatory gene expression after already 2 weeks in LDLr-/- mice, whereas the same diet without cholesterol hardly had an effect on liver inflammation [29]. High-fat diets without cholesterol supplementation induce liver inflammation typically at a slower pace

and, importantly, this liver inflammation is at least partly mediated by the inflamed white adipose tissue (WAT) [5]. However, it is unclear to which extent WAT may contribute to liver inflammation when cholesterol is added to a high-fat diet.

We found that eWAT is more susceptible to develop chronic inflammation than mWAT or iWAT. This observation may be related to the fact that adipocytes in eWAT are more prone to hypertrophy than those in other adipose depots [30]. In the present study, CLS numbers in eWAT correlated with adipocyte size supporting the importance of adipocyte hypertrophy in the development of WAT inflammation [6-8]. Consistent with this, metabolically healthy obese subjects were found to have significantly smaller adipocytes compared with metabolically unhealthy obese patients who had more ectopic liver fat at a comparable body mass index [31]. This suggests that the ability to expand WAT through mechanisms of adipocyte hyperplasia may prevent: a) WAT inflammation and b) ectopic fat accumulation, thereby contributing to a healthy metabolic state.

We observed that rosiglitazone stimulated hyperplasia specifically in subcutaneous WAT thereby preventing adipocyte hypertrophy, which is also observed in patients treated with thiazolidinediones [32,33]. Consequently, this depot did not become inflamed even though its mass was much greater than in control animals, as is seen in humans treated with rosiglitazone.[34] The observed stimulation of hyperplasia specifically in iWAT by rosiglitazone may be explained by depot-specific regulation of perilipin, which is essential for enlargement of lipid droplets. Kim and co-workers showed that perilipin protein expression increased after rosiglitazone treatment in subcutaneous adipose tissue, but did not change in visceral adipose tissue [35].

Clinical trials have shown that treatment with thiazolidinediones can improve liver histology in patients with NASH [36,37]. However, the underlying mechanisms mediating the beneficial effects of thiazolidinediones in NASH development are unclear. Data from the present study support the view that rosiglitazone may attenuate the development of NAFLD via an effect on WAT. Several studies showed that infiltration of macrophages into WAT is strongly associated with NAFLD development [10,38,39]. More specifically, an increase in CD11c+CD206+and CCR2+ macrophages in WAT is associated with enhanced production of pro-inflammatory

adipokines and cytokines in WAT, and NASH severity [39]. Herein we show that rosiglitazone intervention reduced the expression of pro-inflammatory M1 markers, CD11c and CCR2 and increased the expression of anti-inflammatory M2 marker, Arginase-1. An increase in Arginase-1 expression has also been observed in HFD-fed Sv129 mice after treatment with rosiglitazone, but rosiglitazone did not alter the expression of CD11c which may be related to the relatively short intervention period [17]. Long-term rosiglitazone treatment in ob/ob mice resulted in lower CD11c expression level in WAT [40], which is consistent with our findings. Analysis of CLS in the present study shows that long-term rosiglitazone intervention attenuates WAT inflammation by reducing CLS numbers (Figure 2B), rather than altering the activation state of immune cells within a CLS (as determined CD11c and CCR2 immunoreactivity).

Our study indicates that the hepatoprotective effects on NASH by rosiglitazone may at least partly be mediated by adipokines, since plasma leptin and TNFα levels were reduced and plasma adiponectin levels were increased. It is known that leptin can exert pro-inflammatory effects and can activate hepatic stellate cells thereby promoting fibrosis [41]. TNFα plays a crucial role in human and animal NAFLD and neutralization of TNFα activity attenuated the disease.[42] For instance, adiponectin is a potent TNFα-neutralizing cytokine that counteracts inflammation that is relevant for NASH progression [41,42]. It has been demonstrated that also saturated fatty acids can activate inflammatory cascades leading to activation of TNFα.[43] We found that the saturated fatty acids; palmitic acid and stearic acid, were markedly increased by high-fat feeding and reduced with rosiglitazone. Notably, these fatty acids are also increased in patients with diagnosed NASH [44]. Furthermore, surgical excision of inflamed WAT in mice lowered palmitic acid in plasma and reduced progression towards NASH [5]. *In vitro* experiments have shown that conditioned medium from palmitic acid-treated hepatocytes induces the expression of pro-fibrotic genes in hepatic stellate cells [45], providing mechanistic support for a crucial role of inflammatory lipid mediators in NASH. We also observed that rosiglitazone attenuated the HFD-induced hepatic expression of the genes encoding for Col1A1, Col1A2 and TIMP-1. This hepatoprotective effect of rosiglitazone was further substantiated by an effect on genes that are associated

with severity of human NAFLD as shown by Moylan et al [22]. These findings support the view that the experimental conditions established herein (HFD-induced obesity, hyperinsulinemia, WAT inflammation concurrent with histologic NASH) may facilitate preclinical research that aims at translation to the human setting.

In all, intervention with rosiglitazone reduces WAT inflammation, lowers circulating inflammatory mediators and attenuates NAFLD progression. These effects were independent of total adiposity and body weight, indicating that adipose tissue quality (i.e. inflammatory state) rather than absolute mass is critical for NAFLD development. Our results suggest that intervention in WAT may present a new therapeutic option for the treatment of NAFLD.

ACKNOWLEDGEMENTS

The authors would like to thank Erik Offerman, Wim van Duyvenvoorde, Karin Toet, Elvira Fluitsma and Anne Schwerk for their excellent technical assistance. This study was supported by the TNO research programs ‘Enabling Technology Systems Biology’ and ‘Predictive Health Technologies’.

REFERENCES

1. Ng M, Fleming T, Robinson M, Thomson B, Graetz N, Margono C, et al. Global, regional, and national prevalence of overweight and obesity in children and adults during 1980-2013: a systematic analysis for the Global Burden of Disease Study 2013. Lancet 2014;384:766-781.
2. Hotamisligil GS. Inflammation and metabolic disorders. Nature 2006;444:860-867.
3. Lumeng CN, Saltiel AR. Inflammatory links between obesity and metabolic disease. The Journal of clinical investigation 2011;121:2111-2117.
4. Tilg H, Moschen AR. Insulin resistance, inflammation, and non-alcoholic fatty liver disease. Trends Endocrinol Metab 2008;19:371-379.
5. Mulder P, Morrison MC, Wielinga PY, van Duyvenvoorde W, Kooistra T, Kleemann R. Surgical removal of inflamed epididymal white adipose tissue attenuates the development of non-alcoholic steatohepatitis in obesity. International journal of obesity 2015.
6. Bays HE, Gonzalez-Campoy JM, Bray GA, Kitabchi AE, Bergman DA, Schorr AB, et al. Pathogenic potential of adipose tissue and metabolic consequences of adipocyte hypertrophy and increased visceral adiposity. Expert review of cardiovascular therapy 2008;6:343-368.
7. Skurk T, Alberti-Huber C, Herder C, Hauner H. Relationship between adipocyte size and adipokine expression and secretion. The Journal of clinical endocrinology and metabolism 2007;92:1023-1033.
8. Cinti S, Mitchell G, Barbatelli G, Murano I, Ceresi E, Faloia E, et al. Adipocyte death defines macrophage localization and function in adipose tissue of obese mice and humans. Journal of lipid research 2005;46:2347-2355.
9. Fabbrini E, Sullivan S, Klein S. Obesity and nonalcoholic fatty liver disease: biochemical, metabolic, and clinical implications. Hepatology 2010;51:679-689.
10. Kolak M, Westerbacka J, Velagapudi VR, Wagsater D, Yetukuri L, Makkonen J, et al. Adipose tissue inflammation and increased ceramide content characterize subjects with high liver fat content independent of obesity. Diabetes 2007;56:1960-1968.
11. Mirza MS. Obesity, Visceral Fat, and NAFLD: Querying the Role of Adipokines in the Progression of Nonalcoholic Fatty Liver Disease. ISRN gastroenterology 2011;2011:592404.
12. Tilg H, Moschen AR. Adipocytokines: mediators linking adipose tissue, inflammation and immunity. Nature reviews Immunology 2006;6:772-783.
13. Olefsky JM, Glass CK. Macrophages, inflammation, and insulin resistance. Annual review of physiology 2010;72:219-246.
14. Kolak M, Yki-Jarvinen H, Kannisto K, Tiikkainen M, Hamsten A, Eriksson P, et al. Effects of chronic rosiglitazone therapy on gene expression in human adipose tissue in vivo in patients with type 2 diabetes. The Journal of clinical endocrinology and metabolism 2007;92:720-724.
15. Xu H, Barnes GT, Yang Q, Tan G, Yang D, Chou CJ, et al. Chronic inflammation in fat plays a crucial role in the development of obesity-related insulin resistance. The Journal of clinical investigation 2003;112:1821-1830.
16. Nguyen MT, Chen A, Lu WJ, Fan W, Li PP, Oh DY, et al. Regulation of chemokine and chemokine receptor expression by PPARgamma in adipocytes and macrophages. PloS one 2012;7:e34976.
17. Stienstra R, Duval C, Keshtkar S, van der Laak J, Kersten S, Muller M. Peroxisome proliferator-activated receptor gamma activation promotes infiltration of alternatively

activated macrophages into adipose tissue. The Journal of biological chemistry 2008;283:22620-22627.
18. Radonjic M, Wielinga PY, Wopereis S, Kelder T, Goelela VS, Verschuren L, et al. Differential effects of drug interventions and dietary lifestyle in developing type 2 diabetes and complications: a systems biology analysis in LDLr-/- mice. PloS one 2013;8:e56122.
19. Liang W, Menke AL, Driessen A, Koek GH, Lindeman JH, Stoop R, et al. Establishment of a general NAFLD scoring system for rodent models and comparison to human liver pathology. PloS one 2014;9:e115922.
20. Liang W, Tonini G, Mulder P, Kelder T, van Erk M, van den Hoek AM, et al. Coordinated and interactive expression of genes of lipid metabolism and inflammation in adipose tissue and liver during metabolic overload. PloS one 2013;8:e75290.
21. Tiniakos DG, Vos MB, Brunt EM. Nonalcoholic fatty liver disease: pathology and pathogenesis. Annual review of pathology 2010;5:145-171.
22. Moylan CA, Pang H, Dellinger A, Suzuki A, Garrett ME, Guy CD, et al. Hepatic gene expression profiles differentiate presymptomatic patients with mild versus severe nonalcoholic fatty liver disease. Hepatology 2014;59:471-482.
23. Liang W, Lindeman JH, Menke AL, Koonen DP, Morrison M, Havekes LM, et al. Metabolically induced liver inflammation leads to NASH and differs from LPS- or IL-1beta-induced chronic inflammation. Laboratory investigation; a journal of technical methods and pathology 2014;94:491-502.
24. Moran-Salvador E, Lopez-Parra M, Garcia-Alonso V, Titos E, Martinez-Clemente M, Gonzalez-Periz A, et al. Role for PPARgamma in obesity-induced hepatic steatosis as determined by hepatocyte- and macrophage-specific conditional knockouts. FASEB journal : official publication of the Federation of American Societies for Experimental Biology 2011;25:2538-2550.
25. He W, Barak Y, Hevener A, Olson P, Liao D, Le J, et al. Adipose-specific peroxisome proliferator-activated receptor gamma knockout causes insulin resistance in fat and liver but not in muscle. Proceedings of the National Academy of Sciences of the United States of America 2003;100:15712-15717.
26. Gavrilova O, Haluzik M, Matsusue K, Cutson JJ, Johnson L, Dietz KR, et al. Liver peroxisome proliferator-activated receptor gamma contributes to hepatic steatosis, triglyceride clearance, and regulation of body fat mass. The Journal of biological chemistry 2003;278:34268-34276.
27. Gupte AA, Liu JZ, Ren Y, Minze LJ, Wiles JR, Collins AR, et al. Rosiglitazone attenuates age- and diet-associated nonalcoholic steatohepatitis in male low-density lipoprotein receptor knockout mice. Hepatology 2010;52:2001-2011.
28. Wouters K, van Gorp PJ, Bieghs V, Gijbels MJ, Duimel H, Lutjohann D, et al. Dietary cholesterol, rather than liver steatosis, leads to hepatic inflammation in hyperlipidemic mouse models of nonalcoholic steatohepatitis. Hepatology 2008;48:474-486.
29. Funke A, Schreurs M, Aparicio-Vergara M, Sheedfar F, Gruben N, Kloosterhuis NJ, et al. Cholesterol-induced hepatic inflammation does not contribute to the development of insulin resistance in male LDL receptor knockout mice. Atherosclerosis 2014;232:390-396.
30. Caesar R, Manieri M, Kelder T, Boekschoten M, Evelo C, Muller M, et al. A combined transcriptomics and lipidomics analysis of subcutaneous, epididymal and mesenteric adipose tissue reveals marked functional differences. PloS one 2010;5:e11525.
31. O'Connell J, Lynch L, Cawood TJ, Kwasnik A, Nolan N, Geoghegan J, et al. The relationship of omental and subcutaneous adipocyte size to metabolic disease in severe obesity. PloS one 2010;5:e9997.

32. Boden G, Cheung P, Mozzoli M, Fried SK. Effect of thiazolidinediones on glucose and fatty acid metabolism in patients with type 2 diabetes. Metabolism: clinical and experimental 2003;52:753-759.
33. McLaughlin TM, Liu T, Yee G, Abbasi F, Lamendola C, Reaven GM, et al. Pioglitazone increases the proportion of small cells in human abdominal subcutaneous adipose tissue. Obesity 2010;18:926-931.
34. Smith U, Hammarstedt A. Antagonistic effects of thiazolidinediones and cytokines in lipotoxicity. Biochim Biophys Acta 2010;1801:377-380.
35. Kim HJ, Jung TW, Kang ES, Kim DJ, Ahn CW, Lee KW, et al. Depot-specific regulation of perilipin by rosiglitazone in a diabetic animal model. Metabolism: clinical and experimental 2007;56:676-685.
36. Neuschwander-Tetri BA, Brunt EM, Wehmeier KR, Oliver D, Bacon BR. Improved nonalcoholic steatohepatitis after 48 weeks of treatment with the PPAR-gamma ligand rosiglitazone. Hepatology 2003;38:1008-1017.
37. Belfort R, Harrison SA, Brown K, Darland C, Finch J, Hardies J, et al. A placebo-controlled trial of pioglitazone in subjects with nonalcoholic steatohepatitis. The New England journal of medicine 2006;355:2297-2307.
38. Cancello R, Tordjman J, Poitou C, Guilhem G, Bouillot JL, Hugol D, et al. Increased infiltration of macrophages in omental adipose tissue is associated with marked hepatic lesions in morbid human obesity. Diabetes 2006;55:1554-1561.
39. du Plessis J, van Pelt J, Korf H, Mathieu C, van der Schueren B, Lannoo M, et al. Association of Adipose Tissue Inflammation With Histologic Severity of Nonalcoholic Fatty Liver Disease. Gastroenterology 2015;149:635-648 e614.
40. Prieur X, Mok CY, Velagapudi VR, Nunez V, Fuentes L, Montaner D, et al. Differential lipid partitioning between adipocytes and tissue macrophages modulates macrophage lipotoxicity and M2/M1 polarization in obese mice. Diabetes 2011;60:797-809.
41. Marra F, Lotersztajn S. Pathophysiology of NASH: perspectives for a targeted treatment. Current pharmaceutical design 2013;19:5250-5269.
42. Tilg H. The role of cytokines in non-alcoholic fatty liver disease. Digestive diseases 2010;28:179-185.
43. Shi H, Kokoeva MV, Inouye K, Tzameli I, Yin H, Flier JS. TLR4 links innate immunity and fatty acid-induced insulin resistance. The Journal of clinical investigation 2006;116:3015-3025.
44. de Almeida IT, Cortez-Pinto H, Fidalgo G, Rodrigues D, Camilo ME. Plasma total and free fatty acids composition in human non-alcoholic steatohepatitis. Clinical nutrition 2002;21:219-223.
45. Wobser H, Dorn C, Weiss TS, Amann T, Bollheimer C, Buttner R, et al. Lipid accumulation in hepatocytes induces fibrogenic activation of hepatic stellate cells. Cell research 2009;19:996-1005.

SUPPLEMENTAL DATA

Supplement 1: Effect of rosiglitazone intervention on inflammatory CCR2-positive and CD11c-positive immune cells in adipose tissue

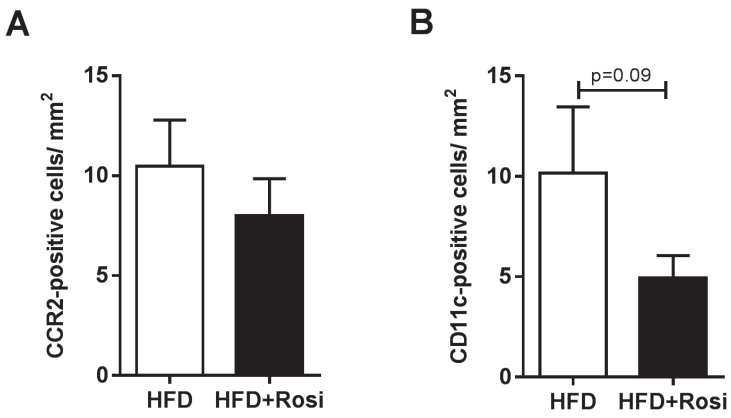

Supplementary Figure 1. To investigate whether rosiglitazone intervention modulates adipose tissue immune cell activation, we have performed immunohistochemical stainings using primary antibodies against CCR2 and CD11c on adipose tissue cross-sections of mice fed a high-fat diet (HFD) or a HFD supplemented with rosiglitazone (HFD+Rosi). We found less immunoreactivity against CCR2 (**Supplementary figure 1A**) and CD11c (**Supplementary figure 1B**) in mice treated with rosiglitazone, which is consistent with the gene expression data. Values are expressed as mean±SEM and expressed as positively stained cells per mm^2 adipose tissue (n=4/group).

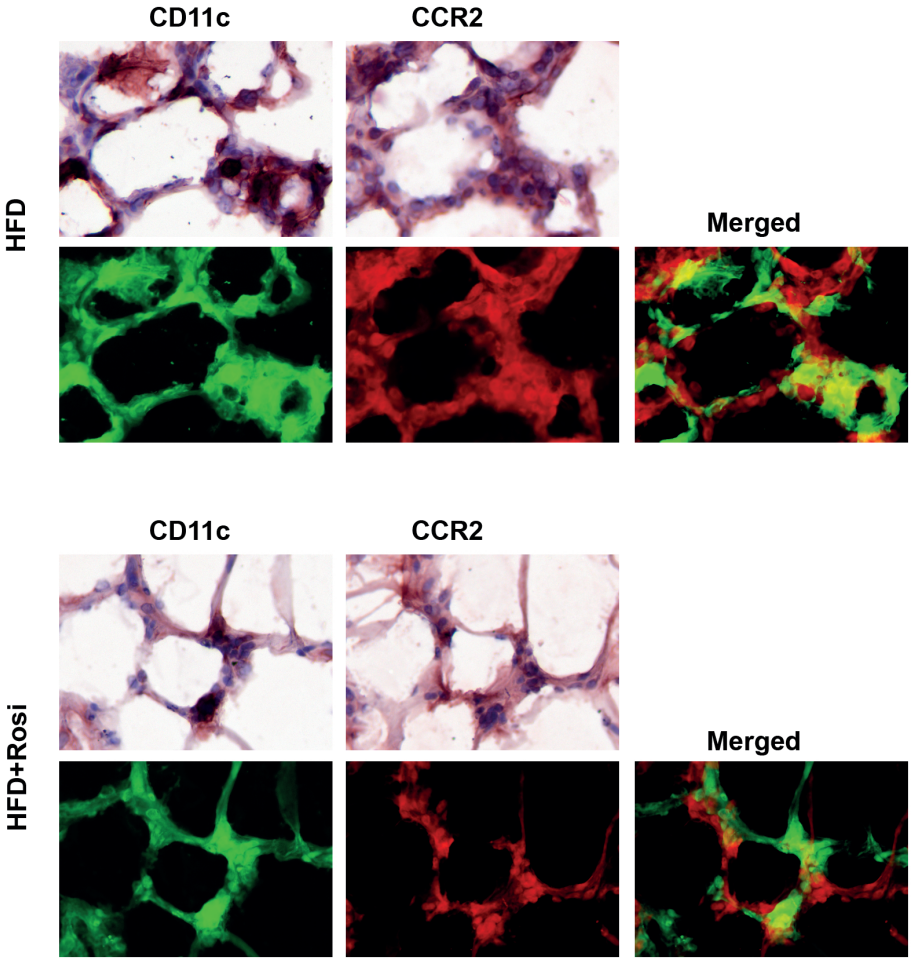

Supplementary Figure 1C shows representative pictures of a crown-like structure (CLS) in adipose tissue of HFD-fed mice and HFD+Rosi mice, which stained positively for CCR2 and CD11c (dark brown staining, upper panels). In order to merge the coloring of the two different immunostainings in a CLS, the bright field images were converted to 8-bit immunofluorescent images (lower panels). The immunoreactivity against CD11c and CCR2 is shown in green and red, respectively. The merged images demonstrate that CLS in the HFD group and the HFD+Rosi group contain CCR2+ and CD11c+ cells and some of these cells express both markers (overlap is indicated by yellow). (Microphotographs: magnification x200).

Supplement 2. Microarray analysis of the effects of rosiglitazone intervention in WAT

Gene set enrichment showed that rosiglitazone intervention significantly affected several biological canonical pathways related to inflammatory oxidative stress in WAT. These pathways can be grouped in three main clusters shown below and specified in **Supplementary Figure 2A-1.**

1. Oxidative phosphorylation/ Mitochondrial dysfunction
2. Oxidative stress response/peroxisomal response
3. Acute phase response/ fibrosis

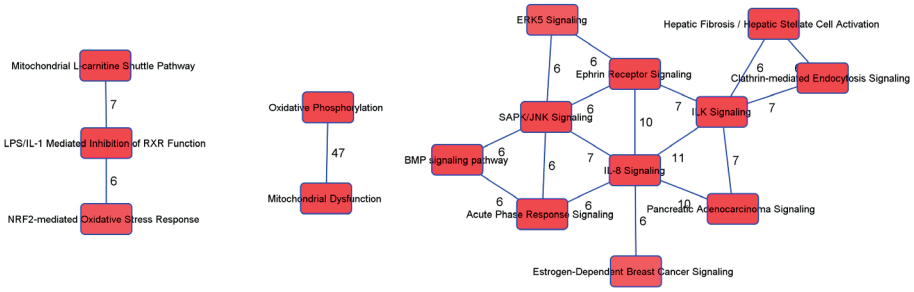

Supplementary Figure 2A-1. Clustering of canonical pathways that are influenced by rosiglitazone intervention. This graph shows three clusters, each of which consisting of canonical pathways. Lines between two pathways indicate that these pathways share genes (the number of overlapping genes is mentioned). The significance of the effect of rosiglitazone on individual pathways is provided in **Supplementary Figure 2A-2.**

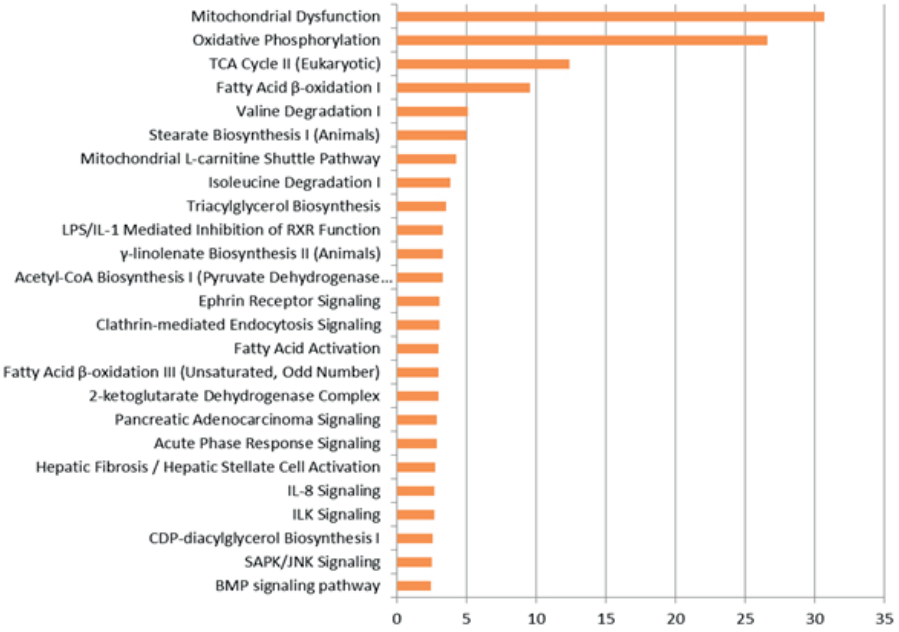

Supplementary Figure 2A-2. **Canonical pathways influenced by rosiglitazone.** The bars in the figure indicate significance of the different pathways. Significance is expressed as -log p-values.

As an example for the anti-inflammatory effect of rosiglitazone in WAT, the individual genes of the canonical pathway 'Acute phase response signaling' are listed in **Supplementary Table 2A**. Among the genes that were reduced by rosiglitazone were complement factors, kinases and acute phase reactants such as haptoglobin, serum amyloid A3 and von Willebrand factor.

Supplementary Table 2A.

Symbol	Entrez Gene Name	Exp Log Ratio	Exp p-value
AGT	angiotensinogen (serpin peptidase inhibitor, clade A, member 8)	-2.45	2.50E-08
C2	complement component 2	-1.345	2.69E-07
C4A/C4B	complement component 4B (Chido blood group)	-1.471	7.47E-09
CFB	complement factor B	-1.856	2.67E-08
HP	haptoglobin	-3.09	4.83E-14
HRAS	Harvey rat sarcoma viral oncogene homolog	0.661	3.62E-03
KRAS	Kirsten rat sarcoma viral oncogene homolog	0.677	7.21E-06
LBP	lipopolysaccharide binding protein	-2.18	8.91E-08
MAPK12	mitogen-activated protein kinase 12	-0.527	5.78E-03
MTOR	mechanistic target of rapamycin (serine/threonine kinase)	0.466	1.13E-03
OSMR	oncostatin M receptor	-0.7	4.47E-05
RBP7	retinol binding protein 7, cellular	2.14	8.13E-09
RELA	v-rel avian reticuloendotheliosis viral oncogene homolog A	-0.417	4.28E-03
RIPK1	receptor (TNFRSF)-interacting serine-threonine kinase 1	-0.276	8.71E-03
RRAS	related RAS viral (r-ras) oncogene homolog	-0.649	1.55E-03
Saa3	serum amyloid A 3	-2.635	3.81E-05
SERPINA3	serpin peptidase inhibitor, clade A (alpha-1 antiproteinase, antitrypsin), member 3	-2.923	3.69E-31
SERPING1	serpin peptidase inhibitor, clade G (C1 inhibitor), member 1	-0.659	7.50E-04
SOCS5	suppressor of cytokine signaling 5	0.455	3.79E-03
TAB1	TGF-beta activated kinase 1/MAP3K7 binding protein 1	-0.415	8.28E-03
TF	transferrin	-0.933	1.07E-04
VWF	von Willebrand factor	-1.115	4.49E-04

Supplementary table 2B. Differentially expressed PPARγ regulated genes in epididymal white adipose tissue affected by rosiglitazone intervention in LDLr-/- mice. Transcriptional network analysis demonstrated a significant transcriptional activation of PPARγ (high and positive Z-score of 4.1, *p*=5.92e-24). Rosiglitazone significantly affected the transcription of 71 PPARγ regulated genes in WAT as listed below. False discovery rate of 5% (FDR<0.05) was used.

Supplementary Table 2B

eWAT	**HFD+Rosi compared with HFD**	
Genes in dataset	**Prediction (based on expression direction)**	**Log Ratio**
UCP1	Activated	3.351
TSC22D3	Activated	-0.799
SORBS1	Activated	0.795
SOD1	Activated	0.542
SLC27A1	Activated	1.810
SLC25A20	Activated	1.399
SLC25A1	Activated	0.991
PPARGC1B	Activated	0.935
PMM1	Activated	1.260
PLIN5	Activated	2.068
PDK4	Activated	3.228
MGLL	Activated	1.015
ME1	Activated	1.048
MDH1	Activated	0.863
HP	Activated	-3.090
HADHB	Activated	1.175
GPD1	Activated	2.167
GDF15	Activated	1.279
FABP5	Activated	1.361
FABP3	Activated	2.700
ESRRA	Activated	0.490
EPHX1	Activated	-0.546
EHHADH	Activated	2.244
DLAT	Activated	1.142
CYP4B1	Activated	1.784
CS	Activated	0.911
CRAT	Activated	1.018
CPT2	Activated	1.249
CPT1B	Activated	3.491
CIDEA	Activated	3.514
CAT	Activated	1.016

Supplementary Table 2B (continued)

eWAT	HFD+Rosi compared with HFD	
Genes in dataset	**Prediction (based on expression direction)**	**Log Ratio**
ATP5O	Activated	1.204
AQP7	Activated	1.205
APP	Activated	-0.551
ACTA2	Activated	-1.767
ACSL1	Activated	1.200
ACOX1	Activated	1.222
ACADS	Activated	1.566
ACADM	Activated	1.035
ACAA2	Activated	1.116
Acaa1b	Activated	1.927
VEGFA	Inhibited	-1.435
PRODH	Inhibited	-1.418
PPIC	Inhibited	-0.959
PPARGC1A	Inhibited	0.934
MLYCD	Inhibited	1.078
LAMB3	Inhibited	-1.329
GATA2	Inhibited	-0.889
ELOVL6	Inhibited	-1.391
CFD	Inhibited	-1.274
CCND1	Inhibited	-0.791
APOE	Inhibited	-0.737
ACSL5	Inhibited	-0.576
Abcb1b	Inhibited	-0.826
ACADL	Affected	1.571
ACOT8	Affected	0.575
AGT	Affected	-2.450
CDK2	Affected	-0.597
FBP2	Affected	1.359
HR	Affected	-1.589
HSD3B7	Affected	-0.842
IGFBP3	Affected	-1.141
IGFBP5	Affected	-1.650
IGFBP7	Affected	-0.404
PDHB	Affected	0.850
S100A8	Affected	-2.150
SCNN1G	Affected	1.209
SCP2	Affected	1.216
UGT1A9 (includes others)	Affected	-1.200
VLDLR	Affected	0.723

Supplement 3: Rosiglitazone intervention does not activate PPAR-regulated genes in livers of LDLr-/- mice

Original transcriptomics data: http://www.ebi.ac.uk/arrayexpress/experiments/E-MTAB-1063/

Supplement 3A: Table listing 36 genes that are differentially expressed by rosiglitazone in liver.

probeID	geneSymbol	geneName	Log Ratio	Adjusted p-value
ILMN_2925947	ABAT	4-aminobutyrate aminotransferase	0.505	4.05E-02
ILMN_2629112	ACER2	alkaline ceramidase 2	0.68	5.03E-03
ILMN_2965414	ANKRD22	ankyrin repeat domain 22	0.94	4.83E-06
ILMN_2834123	APOA4	apolipoprotein A-IV	-2.376	4.48E-03
ILMN_2641301	APOA5	apolipoprotein A-V	-0.823	9.36E-03
ILMN_2732601	ARSG	arylsulfatase G	-0.745	9.36E-03
ILMN_2776603	Ccl9	chemokine (C-C motif) ligand 9	0.621	1.75E-02
ILMN_2835423	CFD	complement factor D (adipsin)	4.666	1.33E-06
ILMN_2609813	CHI3L1	chitinase 3-like 1 (cartilage glycoprotein-39)	1.455	1.88E-02
ILMN_1215446	CIDEA	cell death-inducing DFFA-like effector a	3.387	1.99E-03
ILMN_2827217	CLSTN3	calsyntenin 3	1.349	1.03E-02
ILMN_2806996	CREB3L3	cAMP responsive element binding protein 3-like 3	-0.52	3.19E-03
ILMN_2960325	CTSE	cathepsin E	0.926	3.24E-02
ILMN_2664224	EPHX1	epoxide hydrolase 1, microsomal (xenobiotic)	-0.657	4.60E-02
ILMN_2710698	FGF21	fibroblast growth factor 21	-1.51	2.59E-02
ILMN_2605941	GNPAT	glyceronephosphate O-acyltransferase	0.389	1.67E-02
ILMN_3007956	GZF1	GDNF-inducible zinc finger protein 1	0.398	4.72E-02
ILMN_2795520	HLA-A	major histocompatibility complex, class I, A	-0.523	2.71E-02
ILMN_2662160	IMPA2	inositol(myo)-1(or 4)-monophosphatase 2	-0.779	4.48E-03
ILMN_1229605	INHBE	inhibin, beta E	-0.918	3.24E-02
ILMN_2692723	LPL	lipoprotein lipase	1.261	2.51E-04
ILMN_1225764	MFSD2A	major facilitator superfamily domain containing 2A	-1.977	2.58E-02
ILMN_2813830	NT5E	5'-nucleotidase, ecto (CD73)	0.992	3.69E-02
ILMN_2680628	Pbld2	phenazine biosynthesis-like protein domain containing 2	-0.442	3.20E-02
ILMN_2924754	PDZK1	PDZ domain containing 1	-0.315	7.40E-03
ILMN_1249694	PGM3	phosphoglucomutase 3	-0.536	3.20E-02
ILMN_2739760	PRELP	proline/arginine-rich end leucine-rich repeat protein	-0.429	1.88E-02
ILMN_1254902	RDH16	retinol dehydrogenase 16 (all-trans)	1.318	1.33E-06
ILMN_1240471	RETSAT	retinol saturase (all-trans-retinol 13,14-reductase)	-0.719	1.88E-02
ILMN_2825446	SDCBP2	syndecan binding protein (syntenin) 2	1.575	3.19E-03
ILMN_2684145	SDCBP2	syndecan binding protein (syntenin) 2	0.999	7.40E-03

Supplementary Table 3A (continued)

probeID	geneSymbol	geneName	Log Ratio	Adjusted p-value
ILMN_2826264	SERINC2	serine incorporator 2	-0.72	1.88E-02
ILMN_1231573	SERPINB1	serpin peptidase inhibitor, clade B (ovalbumin), member 1	1.994	4.83E-06
ILMN_1256644	SLC6A12	solute carrier family 6 (neurotransmitter transporter), member 12	0.482	2.58E-02
ILMN_2695199	ST3GAL6	ST3 beta-galactoside alpha-2,3-sialyltransferase 6	0.826	5.02E-05
ILMN_2757599	TSPAN31	tetraspanin 31	-0.415	5.62E-04
ILMN_1236758	WFDC2	WAP four-disulfide core domain 2	-2.028	1.18E-03

Supplement 3B: Specific analysis of PPARγ-regulated genes in liver

Only 4 out of the 36 differentially expressed genes in the liver can potentially be regulated by PPARγ. These 4 genes are listed below. However, also other transcriptional regulators control the expression of these genes and a composite analysis of all gene expression changes (see upstream transcriptional regulator analysis below) shows that PPARγ is not activated.

Supplementary Table 3B

Liver	HFD+Rosi compared with HFD control	
Genes in dataset	**Prediction (based on expression direction)**	**Log Ratio**
CFD	Activated	4.666
CIDEA	Activated	3.387
LPL	Activated	1.276
EPHX1	Activated	-0.657

Supplement 3C: Upstream transcriptional regulator analysis for PPARγ, PPARα and PPARδ in liver

Transcriptional network analysis of differentially expressed genes in liver demonstrated that there is no significant transcriptional activation of upstream regulators PPARγ, PPARα or PPARδ by rosiglitazone. False discovery rate of 5% (FDR<0.05) was used.

As reference for the validity of the method and for PPARα activation, we have used livers from LDLr-/- mice treated with fenofibrate (0.05% w/w), a

pharmacological ligand of PPARα. Diets and duration of intervention were the same as for rosiglitazone. Fenofibrate significantly activates PPARα activity (Z-score: 7.9, *p*=4.5e-55) based on gene expression changes induced by fenofibrate. Consistent with this, a significant activation of several key processes of lipid metabolism in liver was observed with fenofibrate (see **Supplementary Table 3C**). These processes were not affected with rosiglitazone treatment. In line with this, hepatic concentrations of β-hydroxybutyrate (beta-oxidation product) were increased with fenofibrate treatment, but not with rosiglitazone (**Supplementary Figure 3C**), further supporting absence of PPARα activation by rosiglitazone.

Supplementary Table 3C

Top bio functions in lipid metabolism	Predicted Activation State	Log ratio	p-value
transport of long chain fatty acid	Increased	2,902	1,91E-09
oxidation of fatty acid	Increased	2,782	1,04E-17
uptake of long chain fatty acid	Increased	2,634	1,20E-03
storage of lipid	Increased	2,58	3,39E-06

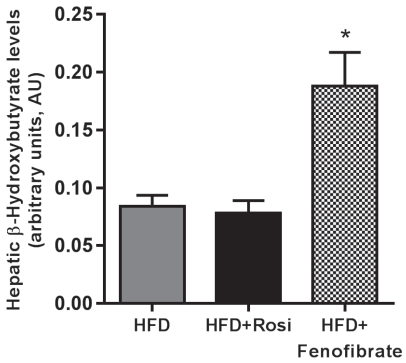

Supplementary figure 3C Using liver tissue homogenates and GC-MS technology, we examined whether rosiglitazone would affect hepatic β-hydroxybutyrate levels (a marker of hepatic fatty acid oxidation) relative to HFD mice. As a positive control for activation of PPARα, livers of fenofibrate-treated LDLr-/- mice were used. The levels of hepatic β-hydroxybutyrate were not increased by rosiglitazone, but were significantly increased by fenofibrate. These data further support absence of PPARα activation by rosiglitazone. Values are expressed as mean ± SEM and expressed as arbitrary units (AU) relative to internal standard. *p<0.05 vs. HFD, HFD+Rosi.

Supplement 4: Effect of rosiglitazone on myeloperoxidase (MPO)-positive cells (neutrophils) in liver

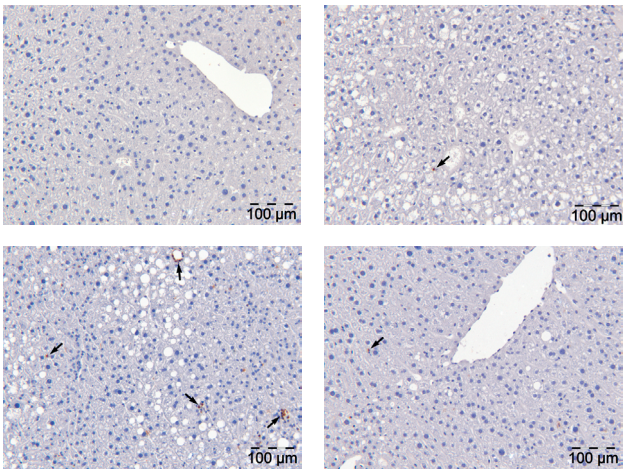

Representative pictures of MPO immunohistochemical stained liver sections of mice after a chow diet (upper left panel), 9 or 16 weeks high-fat diet (REF and HFD, upper right and lower left panel respectively) or rosiglitazone intervention (HFD+Rosi Lower right panel). Infiltration of neutrophils into the liver was observed after 16 weeks of HFD (both single cells and cell aggregates). Only a few MPO-positive cells were observed in HFD+Rosi, which resembled the condition prior to intervention (REF). (magnification x100).

Supplement 5: Effect of rosiglitazone on adipokine plasma concentrations of leptin, TNFα and adiponectin

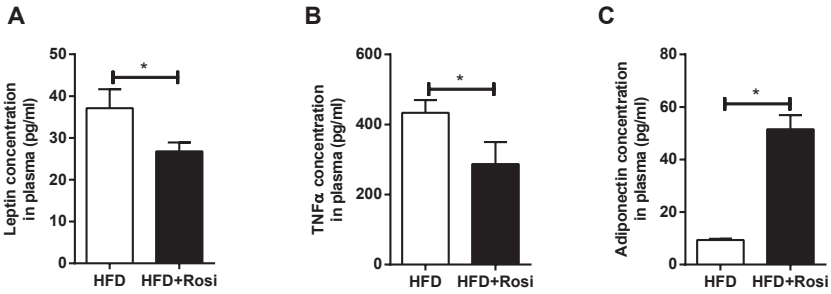

Plasma concentrations of leptin, TNFα and adiponectin of mice fed either a high-fat diet (HFD) or a HFD supplemented with rosiglitazone (HFD+Rosi). Rosiglitazone intervention reduced levels of pro-inflammatory adipokines leptin and TNFα. By contrast, rosiglitazone increased levels of anti-inflammatory adipokine adiponectin. Values are expressed as mean±SEM and expressed as plasma concentrations in pg/ml. *p<0.05.